Computer Networks 56 (2012) 3783–3794

Contents lists available at SciVerse ScienceDirect

Computer Networks

journal homepage: www.elsevier.com/locate/comnet

Rate control for heterogeneous wireless sensor networks: Characterization, algorithms and performance

Jiong Jin [a,*], Marimuthu Palaniswami [a], Bhaskar Krishnamachari [b]

[a] Department of Electrical and Electronic Engineering, The University of Melbourne, Victoria 3010, Australia
[b] Ming Hsieh Department of Electrical Engineering, University of Southern California, Los Angeles, CA 90089, USA

ARTICLE INFO

Article history:
Received 30 September 2011
Received in revised form 21 May 2012
Accepted 28 August 2012
Available online 4 September 2012

Keywords:
Sensor network
Rate control
Resource allocation
Optimization algorithms

ABSTRACT

This paper addresses the rate control and resource allocation problem for heterogeneous wireless sensor networks, which consist of diverse node types or modalities such as sensors and actuators, and different tasks or applications. The performance of these applications, either elastic traffic nature (e.g., typical data collection) or inelastic traffic nature (e.g., real-time monitoring and controlling), is modeled as a utility function of the sensor source rate. The traditional rate control approach, which requires the utility function to be strictly concave, is no longer applicable because of the involvement of inelastic traffic. Therefore, we develop a utility framework of rate control for heterogeneous wireless sensor networks with single- and multiple-path routing, and propose utility fair rate control algorithms, that are able to allocate the resources (wireless channel capacity and sensor node energy) efficiently and guarantee the application performance in a utility proportional or max–min fair manner. Furthermore, the optimization and convergence of the algorithm is investigated rigorously as well.

1. Introduction

With the rapid progress of Wireless Sensor Networks (WSNs), the nature of the network is gradually evolving from *homogeneous* toward *heterogeneous* [1,2]. A *heterogeneous* sensor network consists of various types of nodes such as different sensors (e.g., visual, infra-red, acoustic and camera) and actuators (e.g., robots and mobile entities), and coexists of both low-cost lightweight wireless devices (which simply sense the environmental changes) and energy-rich devices (which serve as in-network or multimedia processors). Compared with a *homogeneous* network, it may contain many different applications associated with particular sensors and integrate all the physical information available to provide rich and versatile services. For instance, heterogeneous sensor network opens up new opportunities in healthcare systems. There is a "smart home" for the disabled and the elderly, with temperature, humidity, pressure sensors and camera deployed. It allows care-providers to monitor patients remotely, react timely and offer a better service. In this case, the applications of heterogeneous sensor networks include not only reactive monitoring operations but also proactive controlling actions.

From the data transport perspective, the objective of heterogeneous sensor networks is no longer to solely maximize the sum of data information collected by each sensor.[1] Instead, it is expected to cater for a variety of application performance metrics related to different sensors or sensor modalities. Rate control (also known as flow control) is an important technique of performance assurance in communication networks. The primary objective of rate control is, by regulating the flows, to prevent network

* Corresponding author. Tel.: +61 3 83440360; fax: +61 3 93471094.
E-mail addresses: jjin@unimelb.edu.au (J. Jin), palani@unimelb.edu.au (M. Palaniswami), bkrishna@usc.edu (B. Krishnamachari).

[1] Hereafter we generally use sensor to refer to all types of sensors including actuators, but differentiate the traffic types by their applications.

1389-1286/$ - see front matter © 2012 Elsevier B.V. All rights reserved.
http://dx.doi.org/10.1016/j.comnet.2012.08.014

congestion with respect to the network capacity. Particularly in wireless sensor networks, there have been numerous proposals (CODA [3], IFRC [4], WRCP [5], RCRT [6]) purely for congestion control. Inspired by the seminal work of Kelly et al. [7], in the past decade, rate control is further adopted to achieve the global network optimality by modeling application performance as a generic utility function over the available bandwidth [8]. Following this model, utility-based rate control has been extensively studied in typical wired networks [9,10], cellular wireless networks [11,12] and ad hoc networks [13,14]. The approach is essentially the same to formulate rate control as an optimization problem and then maximize total utilities under the network bandwidth constraint. Even though this strategy, well known as optimal flow control (OFC), has made a great success in dealing with both congestion control and performance optimization (particularly in proportional fairness), it also possesses serious limitations as outlined in our paper [15,16].

- At current stage, the OFC approach is only suitable for *elastic* traffic, where each application attains a strictly increasing and concave utility function to ensure the feasible optimal solution and convergence of utility maximization process. It cannot deal with congestion control and resource allocation for communication networks like sensor networks where inelastic traffic is commonly engaged.
- In the utility maximization approach, if each user selects different utility function based on its real performance requirement, the OFC approach usually leads to a totally unfair resource allocation for practical use, in particular, an application with a lower demand is conversely allocated with a higher bandwidth.

In this paper, we characterize application performance as a utility function and develop a utility framework of rate control specifically for heterogeneous wireless sensor networks. In order to discriminate different applications regarding different traffic types, hereafter, we relax the utility function conditions, which only require the utility function to be strictly increasing with the data rate, but not necessarily strictly concave. This relaxation has a significant effect on inelastic traffic that is widely existing in sensor networks. Meanwhile, we notice that some models of sensor network simply assume a fixed source rate for sensor node which might not be optimal from a rate control perspective or even not feasible for a given set of resource constraints. Therefore, we study a self-regulating wireless sensor network in which each node is free to adapt its source rate. Then, we design distributed rate control algorithms that allocate source rate among sensor nodes so that the performances of all kinds of sensor nodes are guaranteed. Specifically, we show that the source rate is allocated properly within the sensor networks and that the utility achieved by each node, even not belonging to the same type, is in a proportional or max–min fair manner.

The proposed algorithms target at sensor networks, both with a unique route from each source to a sink and more generally with potentially multiple routes between each sensor node and a sink. The difference is not uncommon in practice due to the availability of a network layer routing protocol [17] that determines unique routes from sources and destinations. Thus, the inclusion of multiple-path scenario is highly desirable from an analytical as well as a practical perspective.

Moreover, unlike traditional wired and wireless networks, sensor networks intrinsically possess some unique characteristics. Energy is a major concern in wireless sensor networks, since the majority of sensor nodes usually have power limited and unreplaceable batteries. We purposely build a power dissipation model and deliberate the energy constraint to make our proposed algorithms energy-aware. It is aimed to guarantee the operational lifetime of sensor networks, which we believe is vitally important.

The rest of the paper is organized as follows: In Section 2, we describe the system models concerning channel capacity constraint and energy constraint. Section 3 discusses the utility framework of rate control for heterogeneous wireless sensor networks. Following that, a utility fair rate control algorithm is designed and developed for single-path network in Section 4 and for multiple-path network in Section 5. Finally, we present the simulation results to evaluate the performances of the proposed algorithms in Section 6 and make conclusions in Section 7.

Notations: Throughout the paper, we use bold lowercase letters $\mathbf{x}, \mathbf{y}, \ldots$ to denote vectors and bold upper-case letters $\mathbf{X}, \mathbf{Y}, \ldots$ to denote matrices. The notations $\mathbb{R}^D$, $\mathbb{R}^D_+$ denote the D-dimensional real and non-negative Euclidean spaces, respectively. Generally, we use the calligraphic font $\mathcal{Z}$ to refer to a set, and the cardinality (i.e., the number of elements) of a finite set $\mathcal{Z}$ is denoted by $|\mathcal{Z}|$.

2. System characterization and modeling

Consider a wireless sensor network that consists of a set $\mathcal{S} = \{1, 2, \ldots, S\}$ of sensor nodes and a single destination node indexed by 0 as sink. In total, there are $K = S + 1$ nodes. Each sensor node s is the source that senses and delivers data information to the sink, possibly over multiple hops. It attains a non-negative utility $U_s(x_s)$ for a source rate $x_s \in [m_s, M_s]$ where m_s and M_s are the minimum and maximum source rate requirements of node s respectively. The utility function $U_s(x_s) : \mathbb{R}_+ \mapsto \mathbb{R}$ is assumed to be continuous, strictly increasing and bounded (not necessarily concave), which indicates the performance of node s. Without loss of generality, it can be assumed that $U_s(x_s) = 0$ when $x_s < m_s$ and $U_s(x_s) = U_s(M_s)$ when $x_s > M_s$. For matters of scalability, it can be further assumed that $0 \leqslant U_s(x_s) \leqslant 1$ and $U_s(M_s) = 1$.

To take account of the network with possible multiple path routing, we assume each sensor node s has n_s available routes or paths[2] from the source to the destination. The total number of paths is $N = n_1 + n_2 + \cdots + n_S$.

Denote the $K \times 1$ vector $\mathbf{r}_{s,i}$ the set of nodes traversed by the path $i \in \{1, 2, \ldots, n_s\}$ originated from node $s \in \mathcal{S}$. Let $y_{s,i}$ be the path rate of sensor node s on path $\mathbf{r}_{s,i}$, and

[2] In the remainder of this paper we will use the terms route and path interchangeably.

$$\mathbf{y} = [y_{1,1}, \ldots, y_{1,n_1}, y_{2,1}, \ldots, y_{2,n_2}, \ldots, y_{S,1}, \ldots, y_{S,n_S}]^{\mathrm{T}} \in \mathbb{R}_+^N$$

be the vector of path rates. Define a matrix $\mathbf{A} \in \{0,1\}^{S \times N}$ such that $\mathbf{A}_{si} = 1$ if and only if the path i is originated from source s, then $\mathbf{x} = \mathbf{A}\mathbf{y}$, where

$$\mathbf{x} = [x_1, x_2, \ldots, x_S]^{\mathrm{T}} \in \mathbb{R}_+^S$$

is the vector of source rates.

2.1. Receiver capacity model and channel capacity constraint

The fundamental difference between designing rate control algorithms for wired and wireless networks is the channel capacity. For wired networks, the notion of capacity is a constant associated with an existing link between any two nodes. For wireless networks, instead of constant, the achievable capacity is largely affected by the interfering links in its vicinity. It therefore requires us to redefine the notion of capacity.

In a wireless network, point-to-point link is replaced by the broadcast domain of each receiver due to its broadcasting nature. It includes all the transmitters within its interference range, which cause interference with each other (Fig. 1a). We thus define the wireless channel capacity in terms of the broadcast domain as the maximum sum rate achievable by flows existing in that broadcast domain and refer to it as *Receiver Capacity* [18,19]. Theoretically, the latest result [19] shows that as long as the receiver capacity is set to 1/3 of the interference free link rate, all rate vectors satisfying the channel capacity constraint by receiver capacity model can be feasibly scheduled. In practice, since most sensor networks use a randomized CSMA MAC as the de facto data link layer, we may simply approximate the capacity of the receiver to the saturation throughput of CSMA MAC. The Receiver Capacity Model is validated through experiments with real wireless devices in [18], and further leads to a practical rate control protocol WRCP in [5].

We further explain the concept of receiver capacity by an illustrative example. Fig. 1b models the interference relationship of Fig. 1a, where the solid line indicates a parent–child relationship in the tree and the dashed line represents an interference link. y_s is the path rate generated at node s being transmitted (in this example, we assume single path routing, so the second subscript of path rate is dropped for simplicity). Rate denoted on the interference link quantifies the amount of interference caused to the affected neighboring node when it is transmitting to its parent. For instance, when node 1 sends its data to node 0 at a certain rate, node 1 not only consumes the corresponding amount of capacity at node 0, but also at node 2; the rate on interference link $1 \rightarrow 2$ is the same as that on link $1 \rightarrow 0$.

Based on this model, we may specify the constraint of the rates at node 1 as follows:

$$y_1^{tot} + y_2^{tot} + y_3 + y_4 \leqslant C_1 \tag{1}$$

where C_1 is the receiver capacity of node 1. y_1^{tot} and y_2^{tot} are the output rates at nodes 1 and 2, respectively, and are given by:

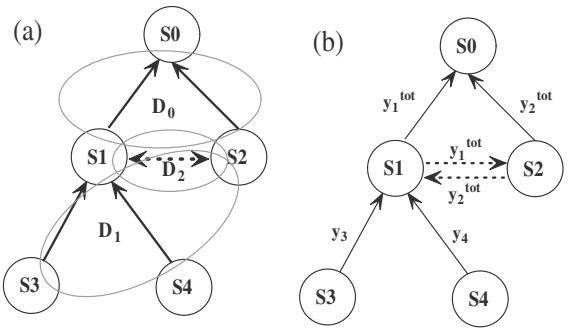

Fig. 1. Receiver capacity model: (a) Broadcast domain and (b) interference representation.

$$y_1^{tot} = y_1 + y_3 + y_4$$
$$y_2^{tot} = y_2$$

Substitute them into Eq. (1), the term y_3 and y_4 are observed to appear twice. One accounts for the consumption of bandwidth during reception at node 1, and the other is as part of the term y_1^{tot} to account for the forwarding of the flows originating at nodes 3 and 4. Essentially, it is because the radio transmission is assumed to be half-duplex. For the rest of the nodes, similar constraints can be listed out.

Given the Receiver Capacity Model, we now present the channel capacity constraint generally. Let $\mathcal{N}_k$ denote the set of all neighbors of node k (including node k itself and all nodes within its interference range); $\mathcal{T}_k$ be the set of paths traversing node k; and C_k be the receiver capacity. The channel capacity constraint at node k is then given as follows:

$$\sum_{s \in \mathcal{N}_k, i \in \mathcal{T}_k} y_{s,i} \leqslant C_k \tag{2}$$

Furthermore, define a matrix $\mathbf{N} \in \{0,1\}^{K \times K}, N_{ij} = 1$ if and only if node j interferes with node i; and a matrix $\mathbf{T} \in \{0,1\}^{K \times N}, T_{ij} = 1$ if and only if path j traverses node i. The channel capacity constraint (2) can then be compactly represented as

$$\mathbf{NTy} \leqslant \mathbf{c} \tag{3}$$

where $\mathbf{c} \in \mathbb{R}_+^K$ is the vector of node receiver capacities.

2.2. Power dissipation model and energy constraint

In the context of sensor networks, nodes are also placed under energy constraint apart from the channel capacity constraint. Typical node operations, such as sensing, transmitting, receiving and relaying data, all consume energy. In this subsection, we introduce the power dissipation model and impose the corresponding energy constraint.

Let e_s, e_t and e_r be the energy consumption per bit incurred in data sensing, transmitting and receiving, respectively. Particularly, e_t includes the radiated energy per bit to ensure reliable communication. In addition, even with low-power listening (lpl) operation [20], there will be energy spent in at least the reception of headers of packets sent by neighboring nodes, even packets that are not to be

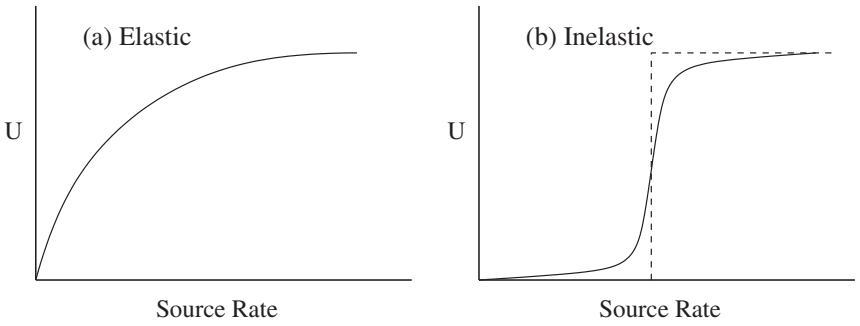

Fig. 2. Utility functions of different traffic types.

forwarded by a given node. Thus, we charge an extra energy term, say $e_h = \rho * e_r$, where $0 \leqslant \rho < 1$ is the ratio of header to total packet size, to all nodes that are within one-hop of the path. In this setting, receivers can sleep all the time but check the header periodically to see if there is some signal on the air for them. If so, they wake up to receive, and otherwise go back to sleep if the packet is not intended.

Define a matrix $\mathbf{E} \in \mathbb{R}_+^{S\times N}$ according to[3]

$$\mathbf{E}_{ij} = \begin{cases} e_s + e_t & \text{if node } i \text{ is the starting node of path } j \\ e_t + e_r & \text{if node } i \text{ is an intermediate node of path } j \\ e_h & \text{if node } i \text{ is within one-hop but not belonging to path } j \\ 0 & \text{otherwise} \end{cases} \tag{4}$$

and let $\mathbf{E}_s$ be the sth row of the matrix $\mathbf{E}$. Note that the energy consumption of computation is neglected as it is much smaller. For a given network flow $\mathbf{y}$, the total energy consumption P_s of node s is $P_s = \mathbf{E}_s\mathbf{y}$.

Next, let B_s denote a limited amount of initial battery (energy) available at node $s, s \in \mathcal{S}$. We define the network lifetime T as the time until the first node in the network runs out of energy as in [21]. By denoting T_s the lifetime of node s, the network lifetime is $T = \min_{s\in\mathcal{S}} T_s$.

Let T_d be the designed network operational lifetime, and also consider the energy consumption of idle listening and sleeping in the lpl mode [20], then

$$B_s = P_s^{\max} T_d + \tau P_{\text{idle}} T_d + (1-\tau) P_{\text{sleep}} T_d. \tag{5}$$

The maximum energy consumption per unit time, or equivalently the maximum power consumption $P_s^{\max}$, allowed at node s for data transportation is hence equal to

$$P_s^{\max} = \frac{B_s}{T_d} - \tau P_{\text{idle}} - (1-\tau) P_{\text{sleep}}, \tag{6}$$

where τ, P_{idle} and P_{sleep} are the duty cycle, power consumed by idle listening and sleeping averaged in a duty cycle, respectively.

To ensure the required network lifetime T_d, the power consumption of each node s should not be more than the maximum allowed power consumption. It leads to the energy constraint for all nodes

$$\mathbf{Ey} \leqslant \mathbf{p} \tag{7}$$

where $\mathbf{p} \in \mathbb{R}_+^S$ is the vector of maximum node power consumptions.

In order to formulate the rate control problem for heterogeneous sensor networks, we first define the notion of feasible (or attainable) path rate allocation.

Definition 1. A source rate is divided into the path rates. Thus, a particular path rate allocation $\mathbf{y} = [y_{1,1}, \ldots, y_{1,n_1}, y_{2,1}, \ldots, y_{2,n_2}, \ldots, y_{S,1}, \ldots, y_{S,n_S}]^{\mathrm{T}} \in \mathbb{R}_+^N$ is *feasible* or *attainable* if and only if the source rate $x_s = \sum_{i=1}^{n_s} y_{s,i}$ for each sensor node s (that is the sum of its available path rates) is within the range $[m_s, M_s]$, and in the sensor network no channel capacity is saturated and no node is energy depleted, i.e.:

$$m_s \leqslant x_s \leqslant M_s,\ s \in \mathcal{S}$$
$$\mathbf{NTy} \leqslant \mathbf{c}$$
$$\mathbf{Ey} \leqslant \mathbf{p}$$

In heterogeneous sensor networks with possible multipath routing, the major task of rate control is to guide the data flows to a feasible path rate allocation, in such a way that each type of sensor application is treated in a fair manner and guaranteed high performance. When resources (channel capacity and node energy) are abundant, there is no difficulty in satisfying every application utility. If resources are not sufficient (or even worse are scarce), then there arises a problem of how to allocate the existing resources fairly among competing sensor nodes that have different utility behaviors.

3. Utility framework of rate control

For sensor networks, usually, people concern about sensor source rates and/or data throughput at the sink. However, since heterogeneous sensor networks are composed of different sensor types, there may exist diverse tasks or applications that exhibit different utility behaviors. A more important factor is data-related application performance, which is measured by its utility function. Regardless of the types of sensors, we assume that utility is a function of sensor source rate.

Similar to the paper [8], we observe two types of typical utility functions in heterogeneous sensor networks. The most common application is data collection from information fields. Taking the "smart home" mentioned in the

[3] The sink is assumed to have sufficient energy supply. Thus, energy constraints are normally considered for S sensor nodes.

introduction as an example, the room temperature is periodically measured by temperature sensors and sent back to the control center, so that data can be logged and analyzed. This class of applications has an *elastic* traffic flow, and the utility function can be described as a (strictly) concave increasing function as shown in Fig. 2a. Utility (performance) increases with source rate, but marginal improvement is decreasing.

Another class is *inelastic* traffic, such as real-time tracking by cameras and real-time controlling by actuators in the "smart home", which generally has an intrinsic bandwidth requirement. Different from the elastic traffic flow, it makes sense only when the source rate exceeds a threshold. A reasonable utility description of this class is close to a single step function as shown in Fig. 2b (solid line), which is convex but not concave at low source rates. Some hard real-time applications even require an exact step utility function as in Fig. 2b (dashed line).

It is clear that elastic traffic and inelastic traffic have significantly different utility functions. In heterogeneous sensor networks, different applications with different traffic types provide different valuable information with respect to the environment. Therefore, the rate control algorithm should have the ability to allocate sensor source rates properly in the sense of providing a good performance balance for different applications.

When considering performances of different applications, it may be undesirable to allocate source rates simply according to conventional criteria such as max–min fairness [22] and proportional fairness [7]. Hence, we develop a utility framework of rate control, which allocates source rates of various applications in terms of their utility requirements. This has inspired a new concept of utility max–min fairness [23,24].

Definition 2. A source rate allocation $\mathbf{x}^* = [x_1^*, x_2^*, \ldots, x_S^*]^T$ is utility max–min fair, if it is feasible and for each sensor node s, the utility $U_s(x_s^*)$ cannot be increased while still maintaining feasibility, without decreasing the utility $U_{s'}(x_{s'}^*)$ for some sensor node s' with a lower utility $U_{s'}(x_{s'}^*) \leqslant U_s(x_s^*)$. Max–min fair allocation is recovered with

$$U_s(x_s) = x_s, \quad s = 1, \ldots, S.$$

Another newly proposed criterion for utility-based fairness is utility proportional fairness [15].

Definition 3. A source rate allocation $\mathbf{x}^* = [x_1^*, x_2^*, \ldots, x_S^*]^T$ is utility proportionally fair, if it is feasible and for any other feasible allocation x,

$$\sum_{s\in\mathcal{S}} \frac{x_s - x_s^*}{U_s(x_s^*)} \leqslant 0. \tag{8}$$

The traditional proportional fairness is recovered if $U_s(x_s) = x_s$. The difference between utility proportional fairness and utility max–min fairness is analogous to the difference between (bandwidth) proportional fairness and (bandwidth) max–min fairness. In the following section, we will propose utility fair rate control algorithms to achieve utility-based fairness within heterogeneous sensor networks and study the properties in detail.

4. Utility fair rate control for single-path network

We first consider the rate control problem for the case in which each source has a unique path to the sink possibly going through multiple hops. It assumes there exists an underlying routing protocol, which is responsible for choosing a path between a source and the sink based on a particular routing policy. The unique path assumption implies the matrix $\mathbf{A}$ defined in Section 2 is an identity matrix and $\mathbf{x} = \mathbf{A}\mathbf{y} \Rightarrow \mathbf{x} = \mathbf{y}$, i.e., the source rate allocation and the path rate allocation is simply the same. Next, we present a distributed algorithm to yield a utility fair resource allocation.

4.1. Distributed utility fair rate control algorithm

The utility fair rate control algorithm uses a similar control structure of optimal flow control approach [9], with the help of pricing mechanism. There are two resource price vectors $\alpha \in \mathbb{R}_+^K$, $\beta \in \mathbb{R}_+^S$ associated with the channel capacity constraint and the node energy constraint, respectively. Each node runs a capacity algorithm and an energy algorithm to update the specific resource price. Concretely, the capacity price depends on the saturation of channel bandwidth usage and the energy price depends on the depletion of node power level. Meanwhile, each end-sensor node runs a source algorithm to adapt the source rate based on these two prices.

Both the capacity algorithm and energy algorithm are iterative. At time $t+1$, the capacity price α_k is updated according to:

$$\alpha_k(t+1) = [\alpha_k(t) + \gamma(x^k(t) - C_k)]^+ \tag{9}$$

where $\gamma > 0$ is a small step size, and $x^k(t) = \sum_{i\in\mathcal{N}_k}\sum_{s\in\mathcal{T}_i} x_s$ is the aggregate source rate at receiver node k. Eq. (9) implies that if the aggregate source rate at node k exceeds the receiver capacity C_k, the capacity price will increase; otherwise it will decrease. The projection $[z]^+ = \max\{0, z\}$ ensures that the capacity price is always non-negative.

Similarly, the energy price β_k is updated at time $t+1$ according to:

$$\beta_k(t+1) = [\beta_k(t) + \gamma(\mathbf{E}_k x(t) - P_k^{\max})]^+ \tag{10}$$

where $\gamma > 0$ is the same step size as Eq. (9), and $\mathbf{E}_k x(t)$ is energy consumption at node k. Eq. (10) also implies that if energy consumption at node k exceeds the maximum power allowed, the energy price will increase; otherwise it will decrease.

Given these two resource prices, each sensor node adopts the following source algorithm to update the source rate:

$$x_s(t+1) = U_s^{-1}\left(\left[\frac{1}{h^s(t)}\right]_{U_s(m_s)}^{U_s(M_s)}\right) \tag{11}$$

where

$$h^s(t) = <\alpha^T\mathbf{T} + \beta^T\mathbf{E}>_s \tag{12}$$

is the sth element of $\alpha^T\mathbf{T} + \beta^T\mathbf{E}$, namely, the aggregate hybrid price of sensor node s, $[z]_a^b = \max\{a, \min\{b, z\}\}$, and U_s^{-1} is the inverse of U_s over the range $[U_s(m_s), U_s(M_s)]$. According

to the definition of utility function, it is clear that $x_s(h^s)$ given by Eq. (11) is decreasing over the hybrid price h^s. When $h^s \geqslant 1/U_s(m_s)$, sensor node s is required to transmit at a minimum rate m_s. When $h^s \leqslant 1/U_s(M_s)$, sensor node s transmits at a maximum rate M_s. In between, source s attains a utility factor of $1/h^s$. Combining (9)–(12), the utility fair rate control algorithm is summarized as follows:

Algorithm 1. At time $t = 1, 2, \ldots$,

1. Update source rate: Each sensor node s calculates the source rate based on the aggregate price of capacity and energy along its path to the sink
$$x_s(t+1) = U_s^{-1}\left(\left[\frac{1}{h^s(t)}\right]_{U_s(m_s)}^{U_s(M_s)}\right)$$
where
$$h^s(t) =< \alpha^T\mathbf{T} + \beta^T\mathbf{E} >_s.$$
2. Update resource prices: Using the aggregate data flow passing through it, each node updates the capacity price α_k and energy price β_k
$$\alpha_k(t+1) = [\alpha_k(t) + \gamma(x^k(t) - C_k)]^+$$
$$\beta_k(t+1) = [\beta_k(t) + \gamma(\mathbf{E}_k x(t) - P_k^{\max})]^+.$$
3. Deliver message towards the sink: Sensor node adapts the updated source rate ($x_s(t+1)$), adds together the capacity price ($\alpha_k(t+1)$) and energy price ($\beta_k(t+1)$) along the path, and propagates towards the sink.
4. Feedback message from the sink: The sink feedbacks the aggregated capacity and energy price to the source via the reverse path individually.

Remark 1. The algorithm that runs on every node in the network requires message exchange in order to form a close-loop control and ensure the optimality of the overall system performance. Instead of communicating individual variables of the algorithm, only the aggregated resource price along each path need to be passed. To achieve low communication overhead, the information could be sent via piggybacking. First, each node collects the local rate information to update both capacity and energy price; then the updated ones are added together with that from the upstream node, and piggybacked onto the data packets of the flows passing by to notify the downstream node along the path. Second, upon the reception, the sink will feedback one aggregated resource price per path to the source by piggybacking onto the acknowledgment packets.

Remark 2. As we know, in the wireless environment, the end-to-end acknowledgment is not always reliable. To further assist information exchange of price-based algorithm, in practice, we may also adopt additional methods such as making use of special control packets [5] or FEEDBACK packets of underlying AODV routing protocol [14].

4.2. Optimization and convergence

The utility fair rate control algorithm (9)–(11) can be viewed as a distributed dual algorithm that solves the following optimization problem:

$$\max_{m_s \leqslant x_s \leqslant M_s} \quad \mathfrak{U}(x) = \sum_{s=1}^{S} \mathfrak{U}_s(x_s) \tag{13}$$

$$\text{s.t.} \quad \mathbf{NTx} \leqslant \mathbf{c} \tag{14}$$

$$\mathbf{Ex} \leqslant \mathbf{p} \tag{15}$$

where

$$\mathfrak{U}_s(x_s) = \int_{m_s}^{x_s} \frac{1}{U_s(y)} dy, \quad m_s \leqslant x_s \leqslant M_s \tag{16}$$

is a "pseudo utility" function for sensor node s.

The original utility function $U_s(x_s)$ is non-negative, continuous and strictly increasing over the range $x_s \in [m_s, M_s]$. Therefore, $\mathfrak{U}_s(x_s)$ must be increasing and strictly concave. If the step size γ in Eq. (9) and (10) is selected to be sufficiently small, the sequence $(\mathbf{x}, \boldsymbol{\alpha}, \boldsymbol{\beta})$ generated by the dual algorithm (9)–(11) will solve the maximization problem (13)–(15). Furthermore, if we define

$$\mathbf{H} = \begin{bmatrix} \mathbf{NT} \\ \mathbf{E} \end{bmatrix} = \begin{bmatrix} \mathbf{N} & \mathbf{0} \\ \mathbf{0} & \mathbf{I} \end{bmatrix} \begin{bmatrix} \mathbf{T} \\ \mathbf{E} \end{bmatrix} = \bar{\mathbf{N}}\bar{\mathbf{H}}$$

and

$$\mathbf{w} = \begin{bmatrix} \mathbf{c} \\ \mathbf{p} \end{bmatrix},$$

constraints (14) and (15) can be combined as

$$\mathbf{Hx} \leqslant \mathbf{w} \tag{17}$$

where $\mathbf{H} \in \mathbb{R}_+^{H \times S}$ and $H = K + S$.

Let

$$W = \max_s \sum_h \bar{\mathbf{H}}_{h,s} \tag{18}$$

$$V = \max_h \sum_s \bar{\mathbf{H}}_{h,s} \tag{19}$$

$$\phi_1 = \max_{s \in \mathcal{S}} \max_{m_s \leqslant x_s \leqslant M_s} U_s(x_s) = \max_{s \in \mathcal{S}} U_s(M_s) \tag{20}$$

$$\phi_2 = \min_{s \in \mathcal{S}} \min_{m_s \leqslant x_s \leqslant M_s} U_s'(x_s) > 0 \tag{21}$$

We now state the main result regarding the convergence of the algorithm.

Theorem 1. *Suppose the step size γ is selected to be*

$$0 < \gamma < \frac{2\phi_2}{\phi_1^2 \sqrt{H} KWV},$$

then the sequence $(\mathbf{x}(t), \boldsymbol{\alpha}(t), \boldsymbol{\beta}(t))$ generated by the utility fair rate control algorithm (9)–(11) will converge to a limit point $(\mathbf{x}^*, \boldsymbol{\alpha}^*, \boldsymbol{\beta}^*)$, where $\mathbf{x}^*$ is the unique optimal solution for the maximization problem (13)–(15).

Proof. The proof is given in the appendix. □

4.3. Utility proportional fairness

When the utility fair rate control algorithm (9)–(11) converges to the equilibrium $(\mathbf{x}^*, \alpha^*, \beta^*)$, the objective function (13) is maximized within the feasible solution. For all feasible allocation $\mathbf{x} \neq \mathbf{x}^*$, the optimality condition is

$$\sum_{s\in\mathcal{S}}\frac{\partial \mathfrak{U}_s(x_s^*)}{\partial x_s}(x_s-x_s^*)=\sum_{s\in\mathcal{S}}\frac{x_s-x_s^*}{U_s(x_s^*)}<0 \tag{22}$$

where the strict inequality follows from the strict concavity of $\mathfrak{U}_s(x_s)$. According to Definition 3, it is clear that, at optimality, the source rate allocation $\mathbf{x}^*$ is utility proportionally fair.

4.4. Utility max–min fairness

The utility max–min fair flow control algorithm initially proposed in [23] is not distributive and each link must be aware of the utility functions from all other sources that traverse such a link. Here we give a new distributive algorithm to achieve the same objective.

For each sensor node s, if the aggregate price is redefined as

$$h^s(t)=\max\{\max_{k\in\mathbf{r}_s}\alpha_k(t),\max_{k\in\mathbf{r}_s}\beta_k(t)\} \tag{23}$$

which takes the maximum of the capacity prices and energy prices along the path, the rate control algorithm (9)–(11) will yield a utility max–min fair allocation within the network.

5. Utility fair rate control for multiple-path network

In this section, we further consider the rate control problem for the network with multipath routing ($\mathbf{A}\neq\mathbf{I}$) and present a distributed algorithm to achieve utility max–min fairness specifically.

5.1. Distributed utility max–min fair rate control algorithm

Since there are possibly multiple paths between each sensor node and the sink for the multipath routing network, in this case, the source rate is made up of several available path rates. For the path rate, instead of using the dual algorithm as (11), we will adopt to use the following first-order Lagrangian algorithm:

$$y_{s,i}(t+1)=\left[y_{s,i}(t)+\gamma\left(\frac{1}{U_s(x_s(t))}-h^r_{s,i}(t)\right)\right]^+. \tag{24}$$

This gentle and smooth adaptation gives better performance when the information fed back is imperfect [15].

Now, based on Algorithm 1, the utility max–min fair rate control algorithm for multiple paths is given as follows:

Algorithm 2. At time $t=1,2,\ldots$,

1. Update source rate: Each sensor node s calculates the path rates based on the hybrid path price $h^r_{s,i}(t)$ and then updates the source rate accordingly

$$y_{s,i}(t+1)=\left[y_{s,i}(t)+\gamma\left(\frac{1}{U_s(x_s(t))}-h^r_{s,i}(t)\right)\right]^+$$

$$x_s(t+1)=\sum_{i=1}^{n_s}y_{s,i}(t+1)$$

where

$$h^r_{s,i}(t)=\max\{\max_{k\in\mathbf{r}_{s,i}}\alpha_k(t),\max_{k\in\mathbf{r}_{s,i}}\beta_k(t)\}. \tag{25}$$

2. Update resource prices: Using the aggregate data flow passing through it, each sensor node updates the capacity price α_k and energy price β_k as Algorithm 1.
3. Deliver message towards the sink: Sensor node adapts the updated path rate $y_{s,i}(t+1)$ that the node can send, compares and stores the larger capacity price $\alpha_k(t+1)$ or energy price $\beta_k(t+1)$ along the path, and propagates towards the sink.
4. Feedback message from the sink: The sink feedbacks the updated largest resource price to the source via the reverse path individually.

Commonly for multipath networks, the set of feasible path rates $y_{s,i}$ may not be unique, so that the first-order Lagrangian algorithm usually oscillates. This is one of the typical difficulties when dealing with multipath networks. In order to eliminate the undesirable effect and further improve the convergence speed, we introduce another augmented variable $\overline{y}_{s,i}$, called the optimal estimation of path rate $y_{s,i}$. In this way, Eq. (24) is slightly modified through applying the concept of low-pass filtering as

$$\begin{aligned}y_{s,i}(t+1)&=\left[(1-\gamma)y_{s,i}(t)+\gamma\overline{y}_{s,i}(t)+\gamma\left(\frac{1}{U_s(x_s(t))}-h^r_{s,i}(t)\right)\right]^+\\ \overline{y}_{s,i}(t+1)&=(1-\gamma)\overline{y}_{s,i}(t)+\gamma y_{s,i}(t).\end{aligned} \tag{26}$$

From the theory of filtering, at optimality, $y_{s,i}=\overline{y}_{s,i}(t+1)$, and notice that the augmented variable is assisted purely to remove the oscillation without changing the optimal solution of $y_{s,i}$.

5.2. Utility max–min fairness

By revisiting Eq. (24), it is observed that either $\frac{1}{U_s(x_s(t))}=h^r_{s,i}(t)$ or $y_{s,i}(t)=0$ at convergence. If we define $h^{r^*}_s=\frac{1}{U_s(x_s(t))}$ for every source node s, the latter case can be interpreted in another way, that is, when the path price $h^r_{s,i}(t)$ is greater than $h^{r^*}_s$, this particular path is too "expensive" to carry any flow ($y_{s,i}(t)=0$). The above fact establishes Theorem 2.

Theorem 2. *For heterogeneous sensor networks with multipath routing, in steady state, the prices on paths $\mathbf{r}_{s,i}$ that carry positive flows $y_{s,i}>0$ must be minimum, and hence equal, among all available paths $\mathbf{r}_s$ of sensor node s. Moreover, the optimal source rate is given by*

$$x_s^*=\sum_{\mathbf{r}^*_{s,i}\in\mathbf{r}^*_s}y^*_{s,i}=U_s^{-1}\left(\left[\frac{1}{h^{r^*}_s}\right]^{U_s(M_s)}_{U_s(m_s)}\right)\text{ and }y_{s,i}=0\quad\text{if }h^r_{s,i}>h^{r^*}_s$$

where $[z]^b_a=\max(a,\min(b,z))$, path $\mathbf{r}^*_{s,i}$ has the minimum path price $h^{r^*}_{s,i}=h^{r^*}_s$, and $\mathbf{r}^*_s$ defines the set of all minimum price paths $\mathbf{r}^*_{s,i}$ of sensor node s.

It is evident that in steady state, the associated utility U_s of node s is equal to $\frac{1}{h^{r^*}_s}$ when $h^{r^*}_s\in[\frac{1}{U_s(M_s)},\frac{1}{U_s(m_s)}]$. Otherwise, it attains a utility $U_s(m_s)$ of the minimum rate requirement whose value is greater than $\frac{1}{h^{r^*}_s}$ (it cannot be any smaller due to the performance requirement), or a utility $U_s(M_s)$ of the maximum rate requirement whose value is less than

$\frac{1}{h_s^{\max}}$ (it needs not to be increased any further). For this reason, we only need to consider the resource allocation of sensor nodes which attain a normal utility $U_s^* = \frac{1}{h_s^{\max}}$.

Regarding the expression of hybrid path price (Eq. (25)), there is no mathematical distinction between capacity prices and energy prices. In general, they are referred to as resource prices. Let $\mathcal{S}_h$ be the set of sensor nodes which have at least one path rate determined by the resource price h. We first pick out the highest resource price h_1 in the sensor network, then all the sensor nodes $s \in \mathcal{S}_{h_1}$ attain the same utility $U_s = 1/h_1$, which are the smallest allocated utility compared with other nodes. If a node $s \in \mathcal{S}_{h_1}$ was to increase its utility U_s by increasing the source rate x_s, there must be another node $s' \in \mathcal{S}_{h_1}$ that would decrease its rate $x_{s'}$ and utility $U_{s'}$ which is previously equal to U_s. In other words, no node can increase its utility without decreasing another one's within $\mathcal{S}_{h_1}$, i.e., utility max–min fairness is achieved within $\mathcal{S}_{h_1}$.

Next, we pick the second highest resource price h_2. Then all the nodes $s \in \mathcal{S}_{h_2}$ have the same utility $U_s = 1/h_2$. If there is a node $s \in \mathcal{S}_{h_2}$ that increases its rate and utility, then there must be another node $s' \in \mathcal{S}_{h_2} \cup \mathcal{S}_{h_1}$ that would decrease its rate which already has a lower utility $U_{s'} \leqslant U_s$. Thus the utility max–min fairness holds for all nodes within $\mathcal{S}_{h_2} \cup \mathcal{S}_{h_1}$.

If we keep ordering and picking all effective resource prices in the above manner, it is concluded by induction that the source rate allocation of sensor nodes is utility max–min fair and that the global fairness is achieved.

6. Simulation results

In this section, we evaluate through simulations the performances of our proposed rate control algorithms. Fig. 3 depicts the topology of wireless sensor network. It contains seven sensor nodes (S_1–S_7) and a sink (S_0). Each sensor node is able to generate and deliver the data to the sink along a certain path possibly over multiple nodes, i.e., $\mathbf{r}_1 = \{S_1, S_0\}$, $\mathbf{r}_2 = \{S_2, S_0\}$, $\mathbf{r}_3 = \{S_3, S_1, S_0\}$, $\mathbf{r}_4 = \{S_4, S_1, S_0\}$, $\mathbf{r}_5 = \{S_5, S_2, S_0\}$, $\mathbf{r}_6 = \{S_6, S_4, S_1, S_0\}$, $\mathbf{r}_7 = \{S_7, S_4, S_1, S_0\}$ (the second subscript of path is dropped for simplicity due to single-path scenario). Note that we first consider the single-path network, where the unique path is determined by the underlying routing protocol. In addition, S_2 is interfered with S_4, and S_6 is interfered with S_7, which are represented by the dashed lines in Fig. 3.

For heterogeneous sensor networks, sensor nodes may embed different sensor types and run different tasks or applications. It results in different associated utility functions. The utility function of each sensor node is given as: $U_1(x_1)=\log(x_1+1)/\log 11, U_2(x_2)=\log(x_2+1)/\log 11, U_3(x_3)=1/(1+e^{-2(x_3-6)}), U_4(x_4)=1/(1+e^{-2(x_4-4)}), U_5(x_5)=1/(1+e^{-2(x_5-6)})$, $U_6(x_6)=0.1x_6$, and $U_7(x_7)=0.1x_7$. The maximum source rates are set at 10 Kb/s. Fig. 4 illustrates these utility functions. In particular, the logarithmic utility function represents an elastic data flow application whereas the sigmoidal function approximates an inelastic real-time application. The linear utility function corresponds to the application whose satisfaction increases linearly.

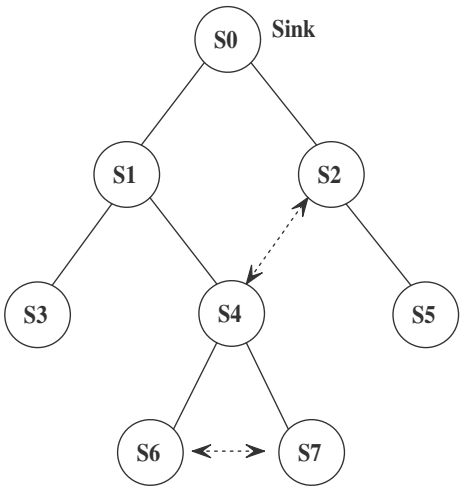

Fig. 3. The topology of wireless sensor network.

We assume a receiver capacity of 80 Kbps, such that it is less than 1/3 of a maximum free link rate of 250 Kbps as in the IEEE 802.15.4 Standard [25] to ensure the feasibility of scheduling. The maximum node power consumption is set to be 9 mW. The parameters e_s, e_t and e_r of the Power Dissipation Model (4) are set to be 100 nJ/bit, 150 nJ/bit, and 158 nJ/bit, respectively, based on the IEEE 802.15.4-compliant CC2420 [26] RF transceiver power dissipation measurements. ρ is set to be 0.2.

In the case of single-path network simulation, the step size $\gamma = 0.002$ is chosen for the algorithm (9)–(11) to satisfy Theorem 1 and ensure fast convergence. The simulation consists of two stages:

- Stage C1.1: iteration $0 \rightarrow 3000$, utility proportional fairness is targeted and the aggregate hybrid price (12) is defined as the sum of the involved resource prices.
- Stage C1.2: iteration $3000 \rightarrow 6000$, utility max–min fairness is deployed and the aggregate hybrid price (23) is defined as the maximum of the involved resource prices.

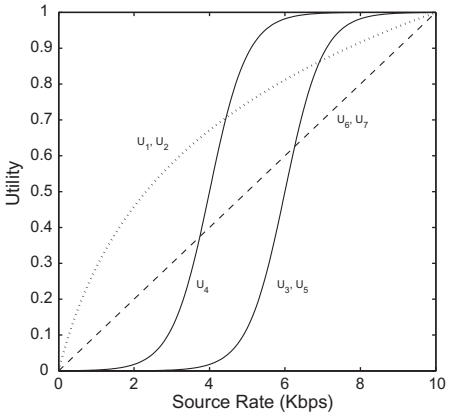

Fig. 4. Sensor nodes utility functions.

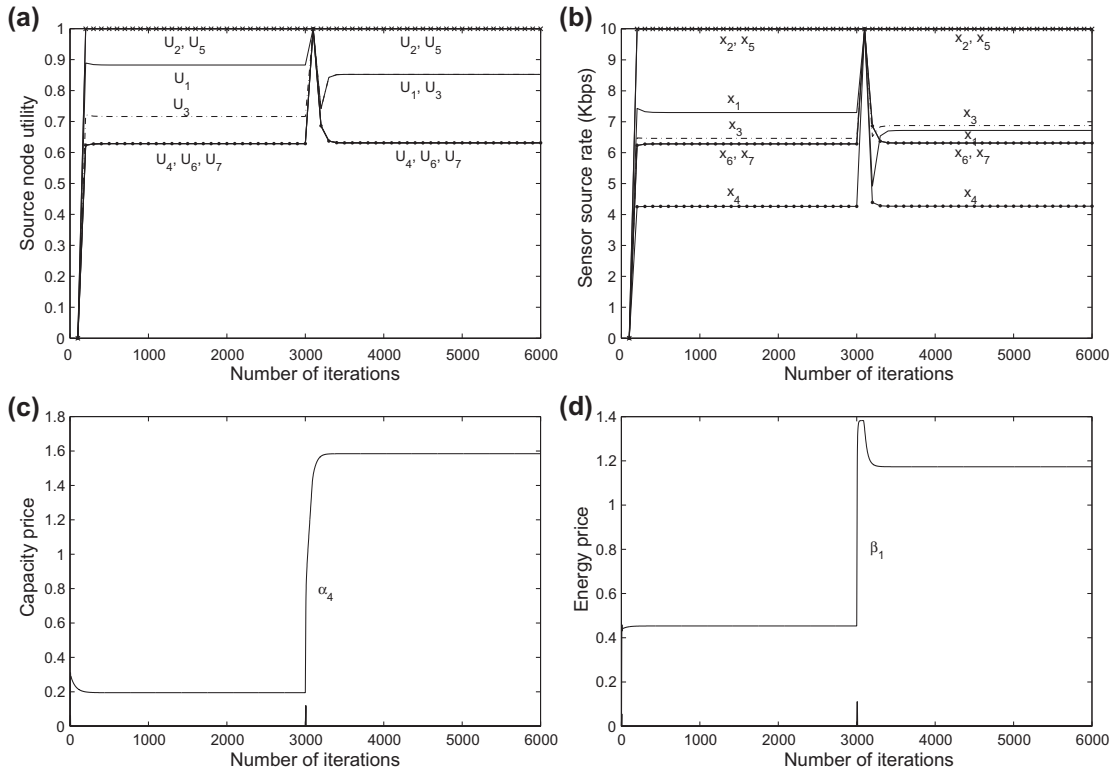

Fig. 5. Simulation results of utility fair rate control algorithm for single-path network: (a) Sensor node utilities, (b) convergence of source rates, (c) capacity prices, and (d) energy prices.

The simulation results are given in Fig. 5a–d. Fig. 5a verifies that the rate control algorithm is efficiently convergent and able to provide either utility proportional or utility max–min fairness in resource allocation among all sensor nodes. Observe from Fig. 5c–d, in equilibrium, except capacity price α_4 and energy price β_1, the remaining resource prices are all equal to zero. By the pricing policy, it can be interpreted that the receiver capacity of S_4 is fully utilized or saturated, and node S_1 is limited by the maximum power consumption constraint. From this perspective, our algorithm successfully takes into account both channel capacity constraint and energy constraint. Especially, for nodes S_4, S_6 and S_7, their utility allocations are the same under Stages C1.1 and C1.2. It is because the sensor source rates are restricted by the receiver capacity constraint of node S_4 all the time.

Next, we carry out the simulation for the case of multiple-path network. Consider the network topology of Fig. 3, node S_4 is also able to communicate directly with node S_2 without the specific routing protocol. Accordingly, S_4, S_6 and S_7 now have two paths each to the sink, i.e., $\mathbf{r}_{4,1} = \{S_4, S_1, S_0\}, \mathbf{r}_{4,2} = \{S_4, S_2, S_0\}, \mathbf{r}_{6,1} = \{S_6, S_4, S_1, S_0\}, \mathbf{r}_{6,2} = \{S_6, S_4, S_2, S_0\}, \mathbf{r}_{7,1} = \{S_7, S_4, S_1, S_0\}, \mathbf{r}_{7,2} = \{S_7, S_4, S_2, S_0\}$.

In this case, we set the step size $\gamma = 0.08$ for Algorithm 2. The simulation also consists of two stages:

- Stage C2.1: iteration $0 \rightarrow 3000$, utility max–min fairness is deployed similarly to the Stage C1.2.
- Stage C2.2: iteration $3000 \rightarrow 6000$, the maximum node power is halved intentionally to prolong the network lifetime as energy is being consumed.

Fig. 6a–d shows the simulation results. They confirm that the proposed rate control algorithm converges rapidly without oscillation in the multipath scenario and properly allocates the source rates to achieve utility max–min fairness in both stages. In Stage C2.1, the nodes S_4, S_6 and S_7 are constrained by the receiver capacity of node S_4 with $U_4 = U_6 = U_7 = 1/\alpha_4 = 0.5312$. In Stage C2.2, since the allowed power consumption is mandatorily reduced to 50%, the sensors in consequence are constrained by the energy (node S_1 and S_2) with $U = 1/\beta_1 = 1/\beta_2 = 0.4512$. It re-enforces the effectiveness of channel capacity constraint and energy constraint. In addition, by comparing the results of Stage C1.2 and Stage C2.1, it is clear that multipath network helps balance the energy better over the whole network.

7. Conclusions

In this paper, we have developed a utility framework of rate control for heterogeneous wireless sensor networks with single- and multiple-path routing. The proposed algorithms are capable of allocating resource for sensor networks, which may contain various sensor types and execute various

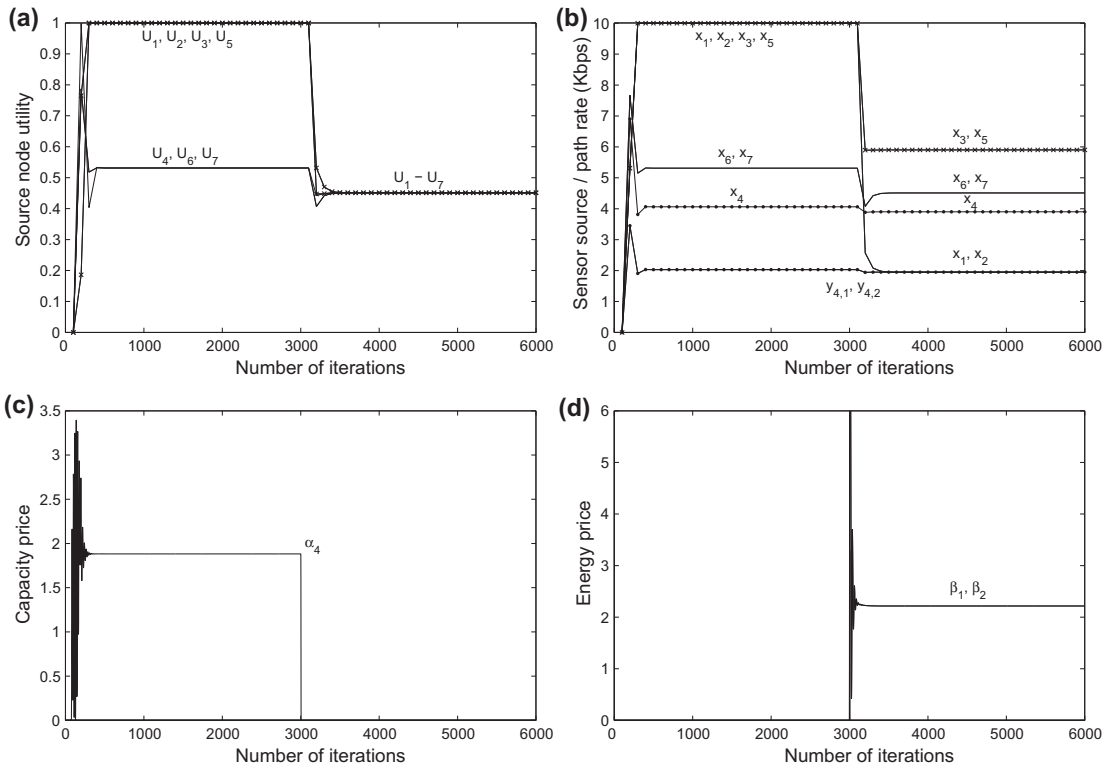

Fig. 6. Simulation results of utility max–min fair rate control algorithm for multiple-path network: (a) Sensor node utilities, (b) convergence of source rates and selected path rates, (c) capacity prices, and (d) energy prices.

tasks. Besides channel capacity constraint, the sensor node energy constraint is also enforced to ensure the designed operational lifetime of sensor networks. We have shown that at convergence, the sensor source rate is properly allocated, and the utility achieved by each node turns into either proportional fairness or max–min fairness. As highlighted, the algorithms presented only require that the sensor node utility function be positive, strictly increasing and bounded over the source rate. It does not require the strict concavity condition on the utility function that is strongly desired by the traditional rate control approach. Therefore, our algorithms are well suited for heterogeneous sensor networks, which commonly carry on inelastic traffic, to provide efficient rate control and fair resource allocation. Moreover, even though the development of this research is in the sensor network setting, the framework generally is extensible to any energy-constrained wireless ad hoc network.

Acknowledgments

This work was supported by the Australian Research Council under Grant No. DP0985322 and ARC Research Networks on Intelligent Sensors, Sensor Networks and Information Processing.

Appendix A. Proof of Theorem 1

In this appendix, we will consistently use vector notations. For a vector $\mathbf{z} = (z_1, z_2, \ldots, z_n)^{\mathrm{T}}$, $||\mathbf{z}||_2$ denotes the Euclidean norm, $||\mathbf{z}||_1 = \sum_i |z_i|$, $||\mathbf{z}||_\infty = \max_i |z_i|$, and $||\mathbf{z}||$ without a subscript denotes any norm. For a matrix $\mathbf{Z}$, $||\mathbf{Z}||$ denotes the correspondingly induced norm.

According to the Lagrangian formulation, the dual function of the optimization problem (13) and (17) is defined as follows:

$$D(\mathbf{h}) = \max_{m_s \leqslant x_s \leqslant M_s} \left(\sum_{s=1}^{S} [\mathfrak{U}_s(x_s) - x_s h^s] + \sum_{h=1}^{H} \mathbf{h}_h \mathbf{w}_h \right) = \sum_{s=1}^{S} [\mathfrak{U}_s(x_s(h^s)) - x_s h^s] + \sum_{h=1}^{H} \mathbf{h}_h \mathbf{w}_h \tag{27}$$

where the hybrid price vector $\mathbf{h} = [\alpha, \beta]^{\mathrm{T}}$, $\mathcal{H}_s$ denotes the nonzero components of sth row of matrix $\mathbf{H}$

$$h^s = \sum_{h \in \mathcal{H}_s} \mathbf{h}_h \tag{28}$$

and

$$x_s(\mathbf{h}) = x_s(h^s) = U_s^{-1} \left(\left[\frac{1}{h^s} \right]_{U_s(m_s)}^{U_s(M_s)} \right) \tag{29}$$

is given by the source algorithm (11) that solves the maximization problem in (27).

The price algorithms (9), (10) can be further viewed as a gradient projection algorithm that solves a dual problem

$$\mathbf{D}: \quad \min_{\mathbf{h} \geqslant 0} D(\mathbf{h}) \tag{30}$$

The following proof is closely related to the proof of Theorem 1 in reference paper [9].

For the property of the dual function $D(\mathbf{h})$, we have the following lemma directly from the definition of $\mathfrak{U}_s(x_s)$.

Lemma 1. *The dual function $D(\mathbf{h})$ is convex, lower bounded and continuously differentiable.*

For any given price vector $\mathbf{h} \geqslant 0$, we define $\chi_s(\mathbf{h})$ by

$$\chi_s(\mathbf{h}) = \begin{cases} \frac{U_s^2(x_s(\mathbf{h}))}{U_s'(x_s(\mathbf{h}))} & \text{if } \frac{1}{U_s(M_s)} \leqslant h^s \leqslant \frac{1}{U_s(m_s)} \\ 0 & \text{otherwise} \end{cases}$$

where $\mathbf{x}(\mathbf{h})$ is given in (29). We will use $x_s(\cdot)$ both as a function of the (scalar) hybrid price h^s and of the vector price $\mathbf{h}$.

Let $\mathbf{X}(\mathbf{h})$ be the $S \times S$ diagonal matrix defined by

$$\mathbf{X}(\mathbf{h}) = Diag(\chi_s(\mathbf{h}), s \in \mathcal{S}) \tag{31}$$

Lemma 2. *The Hessian of D is given by $\nabla^2 D(\mathbf{h}) = \bar{\mathbf{N}}\bar{\mathbf{H}}\mathbf{X}(\mathbf{h})\bar{\mathbf{H}}^{\mathrm{T}}$, where it exists.*

Proof. Let $\frac{\partial \mathbf{x}}{\partial \mathbf{h}}(\mathbf{h})$ denote the $S \times H$ Jacobian matrix whose (s,h) element is $\frac{\partial x_s}{\partial h_h}(\mathbf{h})$. According to (29),

$$\frac{\partial x_s}{\partial h_h}(\mathbf{h}) = \begin{cases} -\frac{U_s^2(x_s(\mathbf{h}))}{U_s'(x_s(\mathbf{h}))}\bar{\mathbf{H}}_{h,s} & \text{if } \frac{1}{U_s(M_s)} \leqslant h^s \leqslant \frac{1}{U_s(m_s)} \\ 0 & \text{otherwise} \end{cases}$$

Using (31) we have

$$\frac{\partial \mathbf{x}}{\partial \mathbf{h}}(\mathbf{h}) = -\mathbf{X}(\mathbf{h})\bar{\mathbf{H}}^{\mathrm{T}} \tag{32}$$

Thus from (27) we have $\nabla D(\mathbf{h}) = \mathbf{w} - \mathbf{H}\mathbf{x}(\mathbf{h})$ and hence

$$\begin{aligned} \nabla^2 D(\mathbf{h}) &= -\mathbf{H}\left(\frac{\partial \mathbf{x}}{\partial \mathbf{h}}(\mathbf{h})\right) = \mathbf{H}\mathbf{X}(\mathbf{h})\bar{\mathbf{H}}^{\mathrm{T}} \\ &= \bar{\mathbf{N}}\bar{\mathbf{H}}\mathbf{X}(\mathbf{h})\bar{\mathbf{H}}^{\mathrm{T}}. \quad \square \end{aligned} \tag{33}$$

Recall W, V, ϕ_1 and ϕ_2 defined in (18)–(21), and we have

Lemma 3. *$\nabla D(\mathbf{h})$ is Lipschitz with*

$$||\nabla D(\mathbf{g}) - \nabla D(\mathbf{h})||_2 \leqslant \frac{\phi_1^2\sqrt{H}KWV}{\phi_2}||\mathbf{g} - \mathbf{h}||_2 \tag{34}$$

for any vector $\mathbf{h}, \mathbf{g} \geqslant 0$.

Proof. Using Lemma 2, we will show that $||\nabla^2 D(\mathbf{h})||_2 = ||\bar{\mathbf{N}}\bar{\mathbf{H}}\mathbf{X}(\mathbf{h})\bar{\mathbf{H}}^{\mathrm{T}}|| \leqslant \frac{\phi_1^2\sqrt{H}KWV}{\phi_2}$. The Lemma then follows from [Theorem 9.19] [27].

With the definition $\mathbf{X}(\mathbf{h})$ in (31),

$$||\nabla^2 D(\mathbf{h})||_2 = ||\bar{\mathbf{N}}\bar{\mathbf{H}}\mathbf{X}(\mathbf{h})\bar{\mathbf{H}}^{\mathrm{T}}||_2 \tag{35}$$

$$\leqslant \frac{\phi_1^2}{\phi_2}||\bar{\mathbf{N}}\bar{\mathbf{H}}\bar{\mathbf{H}}^{\mathrm{T}}||_2 \tag{36}$$

Since (see, [pp. 635] [28])

$$||\bar{\mathbf{H}}\bar{\mathbf{H}}^{\mathrm{T}}||_2^2 \leqslant ||\bar{\mathbf{H}}\bar{\mathbf{H}}^{\mathrm{T}}||_\infty ||\bar{\mathbf{H}}\bar{\mathbf{H}}^{\mathrm{T}}||_1$$

and $\bar{\mathbf{H}}\bar{\mathbf{H}}^{\mathrm{T}}$ is symmetric, $||\bar{\mathbf{H}}\bar{\mathbf{H}}^{\mathrm{T}}||_\infty = ||\bar{\mathbf{H}}\bar{\mathbf{H}}^{\mathrm{T}}||_1$, hence

$$\begin{aligned} ||\bar{\mathbf{H}}\bar{\mathbf{H}}^{\mathrm{T}}||_2 &\leqslant ||\bar{\mathbf{H}}\bar{\mathbf{H}}^{\mathrm{T}}||_\infty \\ &= \max_h \sum_{h'} [\bar{\mathbf{H}}\bar{\mathbf{H}}^{\mathrm{T}}]_{hh'} \\ &= \max_h \sum_{h'} \sum_s \bar{\mathbf{H}}_{h,s}\bar{\mathbf{H}}_{h',s} \\ &\leqslant W \max_h \sum_s \bar{\mathbf{H}}_{h,s} \\ &\leqslant WV \end{aligned}$$

$$||\bar{\mathbf{N}}||_2 \leqslant \sqrt{H}||\bar{\mathbf{N}}||_\infty \leqslant \sqrt{H}K$$

Together with (36), we have (34) which is desirable. $\square$

Since $\mathbf{x}(\mathbf{h})$ in (29) is continuous, the dual function $D(\mathbf{h})$ is lower bounded from Lemma 1 and $\nabla D(\mathbf{h})$ is $\frac{\phi_1^2\sqrt{H}KWV}{\phi_2}$ Lipschitz from Lemma 3. Let $0 < \gamma < \frac{2\phi_2}{\phi_1^2\sqrt{H}KWV}$, any sequence $\mathbf{h}(t)$ generated by the gradient projection algorithm (9) and (10) converges to a limit point $\mathbf{h}^*$, which is the optimal solution for the dual problem **D**. Meanwhile, $\mathbf{x}^* = \mathbf{x}(\mathbf{h}^*)$ is the unique solution for the primal problem (13), (17) (see [28, p. 214]). Thus proof of Theorem 1 is complete.

References

[1] I. Stojmenovic (Ed.), Handbook of Sensor Networks Algorithms and Architectures, Parallel and Distributed Computing, Wiley, 2005.
[2] J. Yick, B. Mukherjee, D. Ghosal, Wireless sensor network survey, Computer Networks 52 (2008) 2292–2330.
[3] C.Y. Wan, S.B. Eisenman, A.T. Campbell, CODA: Congestion detection and avoidance in sensor networks, in: The First ACM Conference on Embedded Networked Sensor Systems, 2003.
[4] S. Rangwala, R. Gummadi, R. Govindan, K. Psounis, Interference-aware fair rate control in wireless sensor networks, in: Proceedings of ACM SIGCOMM Symposium on Network Architectures, Pisa, Italy, September 2006.
[5] A. Sridharan, B. Krishnamachari, Explicit and precise rate control for wireless sensor networks, in: Proceedings of the 7th ACM Conference on Embedded Networked Sensor Systems (SenSys), Berkeley, California, USA, November 2009.
[6] J. Paek, R. Govindan, RCRT: rate-controlled reliable transport for wireless sensor networks, ACM Transactions on Sensor Networks 7(3) (2010).
[7] F.P. Kelly, A. Maulloo, D. Tan, Rate control for communication networks: shadow prices, proportional fairness and stability, Journal of Operations Research Society 49 (3) (1998) 237–252.
[8] S. Shenker, Fundamental design issues for the future Internet, IEEE Journal on Selected Areas in Communications 13 (7) (1995) 1176–1188.
[9] S.H. Low, D.E. Lapsley, Optimization flow control—I: basic algorithm and convergence, IEEE/ACM Transactions on Networking 7 (6) (1999) 861–874.
[10] X. Lin, N.B. Shroff, Utility maximization for communication networks with multipath routing, IEEE Transactions on Automatic Control 51 (5) (2006) 766–781.
[11] C.U. Saraydar, N.B. Mandayam, D.J. Goodman, Pricing and power control in a multicell wireless data network, IEEE Journal on Selected Areas in Communications 19 (10) (2001) 1883–1892.
[12] M. Chiang, S.H. Low, A.R. Calderbank, J.C. Doyle, Layering as optimization decomposition: a mathematical theory of network architectures, Proceedings of the IEEE 95 (1) (2007) 55–312.
[13] Y. Qiu, P. Marbach, Bandwidth allocation in wireless ad hoc networks: A price-based approach, in: Proceedings of IEEE INFOCOM 2003, San Francisco, 2003.
[14] Y. Xue, B. Li, K. Nahrstedt, Optimal resource allocation in wireless ad hoc networks: a price-based approach, IEEE Transactions on Mobile Computing 5 (4) (2006) 347–364.
[15] W.H. Wang, M. Palaniswami, S.H. Low, Application-oriented flow control: fundamentals, algorithms and fairness, IEEE/ACM Transactions on Networking 14 (6) (2006) 1282–1291.

[16] J. Jin, W.H. Wang, M. Palaniswami, Utility max–min fair resource allocation for communication networks with multipath routing, Computer Communications 32 (17) (2009) 1802–1809.
[17] C. Perkins, E. Belding-Royer, S. Das, Ad hoc on-demand distance vector (AODV) routing, RFC3561, July 2003.
[18] A. Sridharan, B. Krishnamachari, Maximizing network utilization with max–min fairness in wireless sensor networks, Wireless Networks (2008).
[19] A. Sridharan, B. Krishnamachari, Feasibility of the receiver capacity model for multi-hop wireless networks, in: Proceedings of the 7th International Symposium on Modeling and Optimization in Mobile, Ad Hoc, and Wireless Networks (WiOpt), 2009.
[20] J. Polastre, J. Hill, D. Culler, Versatile low power media access for wireless sensor networks, in: Proceedings of the 2nd international conference on embedded networked sensor systems (SenSys'04), Baltimore, Maryland, USA, November 2004, pp. 95–107.
[21] J.H. Chang, L. Tassiulas, Energy conserving routing in wireless ad hoc networks, in Proceedings of IEEE INFOCOM 2000, Tel Aviv, Israel, August 2000, pp. 22–31.
[22] D. Bertsekas, R. Gallager, Data Networks, second ed., Prentice-Hall Inc., 1992.
[23] Z. Cao, E.W. Zegura, Utility max–min: an application oriented bandwidth allocation scheme, in: Proceedings of IEEE INFOCOM 1999, March 1999, pp. 793–801.
[24] J. Jin, W.H. Wang, M. Palaniswami, A simple framework of utility max–min flow control using sliding mode approach, IEEE Communications Letters 13 (5) (2009) 360–362.
[25] Wireless Medium Access Control (MAC) and Physical Layer (PHY) specification for low-rate wireless personal area networks, IEEE Computer Society Std. 802.15.4 2003.
[26] CC2420, True single-chip 2.4 GHz IEEE 802.15.4/ZigBee RF transceiver with MAC support, Chipcon Inc. <http://www.chipcon.com>.
[27] W. Rudin, Principles of Mathematical Analysis, third ed., McGraw-Hall Inc., 1976.
[28] D. Bertsekas, J.N. Tsitsiklis, Parallel and Distributed Computation, Prentice Hall, Berlin, 1989.

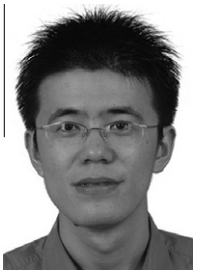

Jiong Jin (IEEE M'11) received the B.E. degree in Computer Engineering from Nanyang Technological University, Singapore, in 2006, and Ph.D. degree from Department of Electrical and Electronic Engineering, the University of Melbourne, Australia, in 2011.
His research interests include control and optimization of the network performance for Internet, wireless ad hoc and sensor networks, flow and congestion control, nonlinear system and sliding mode control theory.

Marimuthu Palaniswami (IEEE F'12) received the B.E. (Hons.) degree from the University of Madras, Chennai, India, the M.E. degree from the Indian Institute of Science, Bangalore, India, the M.Eng.Sc. from the University of Melbourne, Parkville, VIC, Australia, and the Ph.D. degree from the University of Newcastle, Newcastle, Australia.
He has been with the University of Melbourne for over 25 years. He has published more than 320 refereed papers with a majority of them in prestigious IEEE journals and conferences. His research interests are in the fields of computer networks, sensors and sensor networks, machine learning, neural network, pattern recognition, signal processing and control. He is the convener for Australian Research Council Research Network on Intelligent Sensors, Sensor Networks and Information Processing.
Dr. Palaniswami received a Foreign Specialist Award from the Ministry of Education, Japan, in recognition of his contributions to the field of machine learning. He served as associate editor for journals/transactions including IEEE TRANSACTIONS ON NEURAL NETWORKS and Computational Intelligence for Finance. He is the associate editor for the International Journal of Computational Intelligence and Applications and serves on the editorial board of the ANZ Journal on Intelligent Information Processing Systems. He is also the Subject Editor for the International Journal on Distributed Sensor Networks.

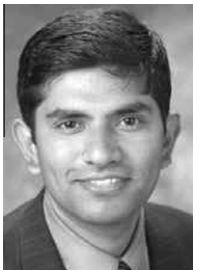

Bhaskar Krishnamachari (IEEE M'02) is Associate Professor and Ming Hsieh Faculty Fellow in the Ming Hsieh Department of Electrical Engineering at the University of Southern California's Viterbi School of Engineering. He received his B.E. from The Cooper Union for the Advancement of Science and Art in 1998, and his M.S. and Ph.D. from Cornell University in 1999 and 2002 respectively, all in Electrical Engineering. He received the U.S. National Science Foundation's CAREER award in 2004, and USC Viterbi School of Engineering's outstanding junior faculty research award in 2005. He has authored a book titled Networking Wireless Sensors, published by Cambridge University Press. His research is focused on modeling, design and analysis of wireless embedded networks.